ORIGINAL RESEARCH

Epothilone B Benefits Nigrostriatal Pathway Recovery by Promoting Microtubule Stabilization After Intracerebral Hemorrhage

Yang Yang, MD; Xuan Zhang, MD; Hongfei Ge, MD; Wei Liu, MD; Eryi Sun, MD; Yuanyuan Ma, MD; Hengli Zhao, MD; Rongwei Li, MD; Weixiang Chen, MD; Jichao Yuan, MD; Qianwei Chen, MD; Yujie Chen, MD, PhD; Xin Liu, PhD; John H. Zhang, MD, PhD; Rong Hu, MD, PhD; Xiaotang Fan, MD, PhD; Hua Feng, MD, PhD

***Background*—**Many previous clinical studies have demonstrated that the nigrostriatal pathway, which plays a vital role in movement adjustment, is significantly impaired after stroke, according to medical imaging and autopsies. However, the basic pathomorphological changes have been poorly investigated to date. This study was designed to explore the pathomorphological changes, mechanism, and therapeutic method of nigrostriatal impairment after intracerebral hemorrhage (ICH).

***Methods and Results*—**Intrastriatal injection of autologous blood or microtubule depolymerization reagent nocodazole was performed to mimic the pathology of ICH in C57/BL6 mice. Immunofluorescence, Western blotting, electron microscopy, functional behavioral tests, and anterograde and retrograde neural circuit tracking techniques were used in these mice. The data showed that the number of dopamine neurons and the dopamine concentration were severely decreased and that fine motor function was impaired after ICH. Microtubule depolymerization was the main contributor to the loss of dopamine neurons and to motor function deficits after ICH, as was also proven by intrastriatal injection of nocodazole. Moreover, administration of the microtubule stabilizer epothilone B (1.5 mg/kg) improved the integrity of the nigrostriatal pathway neural circuit, increased the number of dopamine neurons (4598±896 versus 3125±355; P=0.034) and the dopamine concentration (4.28±0.99 versus 3.08±0.75 ng/mg; P=0.041), and enhanced fine motor functional recovery associated with increased acetylated α-tubulin expression to maintain microtubule stabilization after ICH.

***Conclusions*—**Our results clarified the pathomorphological changes of the nigrostriatal pathway after ICH and found that epothilone B helped alleviate nigrostriatal pathway injury after ICH, associated with promoting α-tubulin acetylation to maintain microtubule stabilization, thus facilitating motor recovery. **(*J Am Heart Assoc*. 2018;7:e007626. DOI: 10.1161/JAHA.117.007626.)**

Key Words: epothilone B • intracerebral hemorrhage • microtubule stabilization • movement disorder • nigrostriatal pathway

Intracerebral hemorrhage (ICH) is an intractable neurological malady with high morbidity and mortality.[1] Despite stable incidence rates and declining mortality rates over the past 2 decades, motor dysfunction remains an intractable problem with no clinically available interventions except rehabilitation.[2] Specifically, basal ganglia hemorrhage leads to significant and severe motor dysfunction owing to the specific anatomic structure, which comprises white matter fiber tracts and the nigrostriatal pathway.[3] However, the basic pathomorphological changes and injury mechanisms of the nigrostriatal pathway, which plays a vital role in movement adjustment,[4] following ICH have been poorly investigated to date. Furthermore, prospective, randomized, and double-blind studies have revealed that the

From the Department of Neurosurgery, Southwest Hospital (Y.Y., X.Z., H.G., W.L., H.Z., R.L., W.C., Q.C., Y.C., X.L., R.H., H.F.), Department of Basic Nursing, School of Nursing (Y.M.), Department of Neurology, Southwest Hospital (J.Y.), and Department of Developmental Neuropsychology, School of Psychology (X.F.), Third Military Medical University, Chongqing, China; Neurosurgery Department of Guizhou Medical University Affiliated Hospital, Guiyang, Guizhou, China (E.S.); Department of Anesthesiology, Neurosurgery and Physiology, Loma Linda University, Loma Linda, CA (J.H.Z.).

Accompanying Figures S1 through S3 are available at http://jaha.ahajournals.org/content/7/2/e007626/DC1/embed/inline-supplementary-material-1.pdf

Correspondence to: Hua Feng, MD, PhD, and Rong Hu, MD, PhD, Department of Neurosurgery, Southwest Hospital, The Third Military Medical University, 29 Gaotanyan Street, Chongqing 400038, China. E-mails: fenghua8888@vip.163.com, huchrong@aliyun.com and Xiaotang Fan, MD, PhD, Department of Developmental Neuropsychology, School of Psychology, Third Military Medical University, 30 Gaotanyan Street, Chongqing 400038, China. E-mail: fanxiaotang2005@163.com

Received November 5, 2017; accepted December 6, 2017.

© 2018 The Authors. Published on behalf of the American Heart Association, Inc., by Wiley. This is an open access article under the terms of the Creative Commons Attribution-NonCommercial License, which permits use, distribution and reproduction in any medium, provided the original work is properly cited and is not used for commercial purposes.

Clinical Perspective

What Is New?

- Intracerebral hemorrhage–induced nigrostriatal pathway injury aggravates motor dysfunction.
- Microtubule depolymerzation contributes to nigrostriatal pathway injury after intracerebral hemorrhage, and treatment with microtubule stabilizer epothilone B alleviates nigrostriatal pathway injury and improves motor function.

What Are the Clinical Implications?

- This microtubule-targeted therapeutic strategy has a translational promise for treating functional recovery after intracerebral hemorrhage, from bench to bedside.

dopamine precursor levodopa, which is administered as an alternative dopaminergic therapeutic strategy, enhances motor recovery in patients with hemiplegia and procedural motor learning disorders after stroke.[5–7] This evidence suggests that protection of the nigrostriatal pathway may confer important benefits in motor recovery after stroke.

Microtubule is a component of the cytoskeleton, and microtubule dynamics participate in many cellular processes, including mechanical support, cell motility, organization of the cytoplasm, and secretory vesicle transport, through repeated polymerization/depolymerization interactions.[8] Recent studies have demonstrated that midbrain dopamine neurons are particularly vulnerable to microtubule depolymerization.[9] Furthermore, research has indicated that striatal injection of the microtubule disruptor colchicine leads to motor dysfunction and dopamine neuron degeneration in the substantia nigra pars compacta (SNc) due to microtubule depolymerization.[10] In addition, studies have revealed that microtubule stabilizing agents (ie, paclitaxel [Taxol; Bristol-Myers Squibb] and epothilone B [epoB]) can maintain axon morphology, promote axon regeneration, and improve motor dysfunction in rodents with either spine cord or optical nerve injury.[11–13] Thus, maintaining microtubule stabilization might be an effective therapy to ameliorate pathological changes in dopamine neurons and to restore motor function after ICH.

In this study, we hypothesized that ICH would lead to significant motor dysfunction in part by impairing nigrostriatal projections caused by microtubule depolymerization and that administration of epoB would alleviate nigrostriatal projections and improve motor function by stabilizing microtubules. This study aimed to further elucidate the pathomorphological changes of nigrostriatal projections and the potential mechanism involved to identify a feasible treatment approach for ICH.

Materials and Methods

The data that support the findings of this study are available from the corresponding author on reasonable request.

Animals

A total of 224 adult male C57/BL6 mice (8–10 weeks, 20–25 g) and 10 pregnant C57/BL6 mice (E16.5) were used in this study and provided by the Experimental Animal Center at the Third Military Medical University. The mice were housed in a specific temperature-controlled room under a standard 12-hour light/dark cycle and provided free access to food and water.

ICH Model

All experimental procedures were approved by the ethics committee of the Third Military Medical University and performed according to the health guide for the care and use of laboratory animals. The ICH model was established in accordance with previously described methods.[14,15] A small cranial burr hole was made at a precise location (bregma coordinates: 0.8 mm anterior and 2 mm lateral to the midline) under stereotactic guidance, and 25 μL autologous blood was injected 3 mm deep into the right basal ganglia at a rate of 2 μL/min using a microinfusion pump. Mice were divided into the following 3 groups: sham, ICH + vehicle (ICH+Veh), and ICH + epoB. The ICH mice received epoB (0.75 or 1.5 mg/kg IP, dissolved in dimethyl sulfoxide [DMSO] and saline at a ratio of 1:3) or an equal volume of vehicle 2 hours after the ICH procedure.

For the microtubule injury model,[16] 10 μL of 100 μmol/L of the microtubule destabilizing agent nocodazole (diluted into 5% DMSO in saline) or 5% DMSO alone was injected into the striatum using a sterile microsyringe. After 2 hours, the microtubule-injured mice were intraperitoneally administered epoB or vehicle. These mice were also divided into 3 groups: sham, nocodazole + vehicle, and nocodazole + epoB. At 1, 3, 7, and 14 days after surgery, the mice underwent functional behavioral tests and were weighed. The mice were then deeply anesthetized, and the brains were collected for morphological and biochemical experiments.

Immunofluorescence

Immunofluorescence was performed according to the method described by Yang et al.[17] Cryostat sections 30 μm thick were incubated with the following primary antibodies in 1% BSA (overnight, 4°C): rabbit anti–tyrosine hydroxylase (anti-TH, 1:1000), mouse anti-TH (1:1000), and rabbit anti–rabbit VMAT2 (vesicular monoamine transporter 2; 1:1000). After the sections were washed with 0.01 mol/L phosphate buffer, they were probed with the appropriate Cy3-, 488-conjugated,

and Cy3-SABC secondary antibodies (1:500, 4 hours, at room temperature). Finally, the sections were counterstained with DAPI (4′,6-diamidino-2-phenylindole) and mounted in Vectashield medium (Vector Laboratories) before being photographed using either a Zeiss Axiovert microscope equipped with a digital color camera or a Zeiss confocal microscope (LSM780; Zeiss).

High-Performance Liquid Chromatography–Electrochemical Detection Analysis

The concentration of dopamine in the impaired striatum and ipsilateral substantia nigra (SN) of the ICH mice was measured using high-performance liquid chromatography–electrochemical detection, as described previously.[18] The chromatographic data were exported and analyzed using ESA software (ESA, Inc). The area under the curve of a standard concentration of dopamine was used to compare the dopamine concentrations in the samples.

Electron Microscopy and Morphometric Analysis

Seven days after autologous blood and nocodazole were injected into the striatum, the mice in each group were processed for electron microscopy analysis, as described previously.[19] After fixation, ultrathin sections (≈60 nm thick) were sliced using an ultramicrotome (LKB-V; LKB Produkter AB) and counterstained with uranyl acetate and lead citrate. These ultrathin sections were viewed under a transmission electron microscope (TECNAI10; Philips), followed by compilation and analysis using Adobe Photoshop and ImageJ (US National Institutes of Health).

Western Blot Analysis

Western blot was performed as described by Xu et al.[18] Total protein was extracted from the brain tissues surrounding the hematoma region and at the ipsilateral SN. After gel electrophoresis and transfer to membranes, the membranes were incubated with the following primary antibodies at 4°C overnight: rabbit anti-TH (1:1000, Millipore), rabbit anti–kinesin heavy chain 2 (1:1000), rabbit anti–cytoplasmic dynein 1 light intermediate chain 1 (1:1000), rabbit anti-VMAT2 (1:1000), rabbit anti-αTAT1 (C6orf134, 1:1000), rabbit anti–acetylated α-tubulin (acetyl K40, acetyl-tubulin, 1:1000), mouse anti–α-tubulin (T-tubulin, 1:1000), and mouse anti-GAPDH (1:2000), which was used as a loading control. Then, the membranes were probed with specific horseradish peroxidase–conjugated secondary antibodies (1:1000) for 3 hours at room temperature. Finally, an enhanced chemiluminescence reagent kit for Western blotting was used to visualize the immunoreactive bands, which were detected with a bioimaging system (VersaDoc MP 4000; Bio-Rad). Three animals from each group and at least 3 repetitions of each treatment condition were used for the Western blot analysis.

White Blood Cell Count

White blood cell counts were measured in blood samples that were collected via sterile caudal vein puncture at 0, 1, 3, 7, and 14 days after ICH. Approximately 100 μL of blood was tested using a Sysmex SYSMEXSF-3000 automated hematology analyzer. The number of white blood cells was recorded for analysis.

Tracking of Anterograde and Retrograde Neural Circuits

A lipophilic carbocyanine dye was used for retrograde neural circuit tracking. The lipophilic membrane retrograde tracer stain DiI (1,1′-dioctadecyl-3,3,3′,3′-tetramethylindocarbocyanine perchlorate; 10 mg/mL in DMSO, 0.5 μL/site) was injected into the ipsilateral striatum (bregma coordinates: 1.34 mm anterior, 2 mm lateral to the midline, and 2.5 mm at depth) in front of the hemorrhagic region 3 days after the ICH operation. After 4 days of tracking, the mice were deeply anesthetized and euthanized for morphological analysis of dopamine neurons.

Classical anterograde neural circuit tracking was implemented using biotin dextran amine (BDA), as described previously.[20] BDA (3–5 sites, total volume is 1 μL, 10 μL/mg in sterile saline) was injected into the SNc area (bregma coordinates: −3 mm anterior, 1 mm lateral to the midline, and 4-mm depth) 3 days after the ICH operation. After 11 days of tracking, mice were euthanized, and the dopamine fibers in the striatum were examined using immunofluorescence staining.

Neurological Scoring

Neurological scores were assessed at 1, 3, 7, and 14 days after ICH according to the method described by Sugawara et al. An 18-point scoring system was used to evaluate the neurological deficits in a double-blind fashion, including spontaneous activity (in cage for 5 minutes), spontaneous movement of all limbs, movement of the forelimbs (outstretching while the animal was held by the tail), climbing the wall of a wire cage, reaction to touch on both sides of the trunk, and response to having the vibrissae touched.

Functional Behavioral Tests

Open-field, beam-walking, rotarod, and ladder-rung walking tests were used to assess the voluntary activities and motor function of the mice at 1, 3, 7, and 14 days after ICH impairment.

Open-field movement was measured using an open-field activity system and analyzed using Noldus EthoVision XT software (Noldus Information Technology Co, Ltd), as described previously.[18]

Beam walking was used to assess fine motor coordination by examining the ability of the animal to remain upright and to walk on a narrow beam.[21] The narrow beam was ≈0.6 cm wide, 120 cm in length, and 60 cm above the soft bedding material. All mice were trained on the beam 1 day before ICH, and only mice whose paws slipped down the horizontal surface of the beam (foot faults) <10 times per 50 steps were used for experiments. The number of contralateral forelimb and hind-limb foot faults within 50 steps were counted and analyzed, and mice that took <50 steps after ICH were excluded.

Similarly, the ladder-rung walking task, which is sensitive to changes in performance during recovery periods, was used to assess the subtle loss of movement capacity.[22] The horizontal ladder-rung walking test apparatus was 100 cm long, 19 cm high, and 10 cm wide. Metal rungs (3-mm diameter) were inserted on clear Plexiglas walls to create a floor with a minimum distance of 1 cm between the rungs; the spacing of the rungs is variable and changed periodically. Before ICH, the animals were trained to learn to walk on the ladder rungs with a regular pattern (1 rung every 1 cm) and to anticipate the position of the rungs. For each experimental trial, irregular patterns (randomly spaced 30 rungs; maximum distance of 3 cm between the rungs) that were changed for each trial were used to prevent the animal from learning the pattern. The correct contralateral forelimb and hind-limb placements within 50 steps were counted and analyzed, and mice who took <50 steps after ICH were excluded.

The rotarod test was used to estimate gross motor deficits and grip strength in the rodents, as described by Fox et al.[23] The speed was set to gradually increase from 5 to 35 rpm in ≈1.5 minutes, and the latency to fall (or cling to and spin with the rod for 3 full rotations) within 3 minutes was recorded for statistical analysis. Three trials for each mouse were performed, separated by 10 minutes. Latency of <60 seconds 1 day before implementing ICH was set as an exclusion criterion for surgery.

Primary Neuronal Culture and Treatment

Time-pregnant mice (C57/BL6) that were bred in house were used to generate prenatal mouse pups for neuronal culture. The day of vaginal plug detection was designated as E0.5. The planned harvest time for culture was E16.5. Primary neurons were isolated and cultured, as described previously, with some modifications.[24] SN and striatal tissues were clearly separated from the mesencephalon, and after digestion, cell suspension was counted and adjusted to 1×10^4 cells per 75 μL of living SN neurons and 2×10^5 cells per 75 μL of living striatal cells. The SN cell suspensions (75 μL) were plated on 12-mm-diameter coverslips precoated with 10 μg/mL poly-L-ornithine, whereas the striatal cell suspensions were plated in a 24-well plate in medium conducive to maintaining SN neuron growth. After 3 days of culture, the primary SN neurons on the coverslips were treated with TH antibody and several intervention factors.

Oxyhemoglobin was selected and added to the primary SN neuron cultures at a concentration of 10 μmol/L in vitro to simulate ICH and 45 nmol/L nocodazole was used as a positive control for microtubule depolymerization. EpoB was added at a concentration of 5 nmol/L, as described previously. Consequently, there were 6 experimental groups: control, epoB, nocodazole, oxyhemoglobin, nocodazole + epoB, and oxyhemoglobin + epoB. After 12 hours in culture, the cells were fixed with 4% paraformaldehyde for analysis.

Short Hairpin RNA Interference and EpoB Local Injection

To investigate whether α-tubulin acetylation on lysine 40 is key for the protective function of epoB, we designed 3 short hairpin RNAs (shRNAs) targeting αTAT1 (α-tubulin K40 acetyltransferase) and 1 scrambled shRNA. The αTAT1 shRNA sequences were 5′-GACATTAAGCCATACTCTT-3′, 5′-GAACAACTTTGTCATCTTT-3′, and 5′-TCCTGAATAAGCACTACAA-3′. Plasmids and lentiviruses were generated. The methods of shRNA interference and quantitative real-time polymerase chain reaction were implemented, as described previously.[25] The primer sequences were as follows: αTAT1, forward primer, GCACTACAACCTGGAGACCACA, reverse primer, GTTGCTCTCAGAGAGGAAGTGG; and GAPDH, forward primer, ATGTTCCAGTATGACTCCACTCACG, reverse primer GAAGACACCAGTAGACTCCACGACA.

Stereotaxic injection of lentiviruses and epoB into the SN area was used for studying the role of acetylated α-tubulin in vivo. Generated recombinant human B lymphotropic virus–αTAT1 shRNA–GFP (green fluorescent protein), human B lymphotropic virus–GFP and epoB (200 ng dissolved in 2 μL solution according to study 1 [DMSO and saline at a ratio of 1:3]) were injected into the SN area. In addition, 1-μL titers of engineered lentivirus (1×10^9 virus particles per mL) solution and 2 μL epoB were delivered to the SN area via stereotaxic injection (bregma coordinates: −3 mm anterior, 1 mm lateral to the midline, and 4 mm depth). The lentiviruses and epoB were injected 2 hours after ICH surgery, and the mice were euthanized for biochemical experiments after 7 days of infection.

Immunoreactivity Quantification

TH-positive cells at the SNc were stereologically estimated in accordance with a previous study.[26] Every sixth section was examined through the entire rostrocaudal extension of the

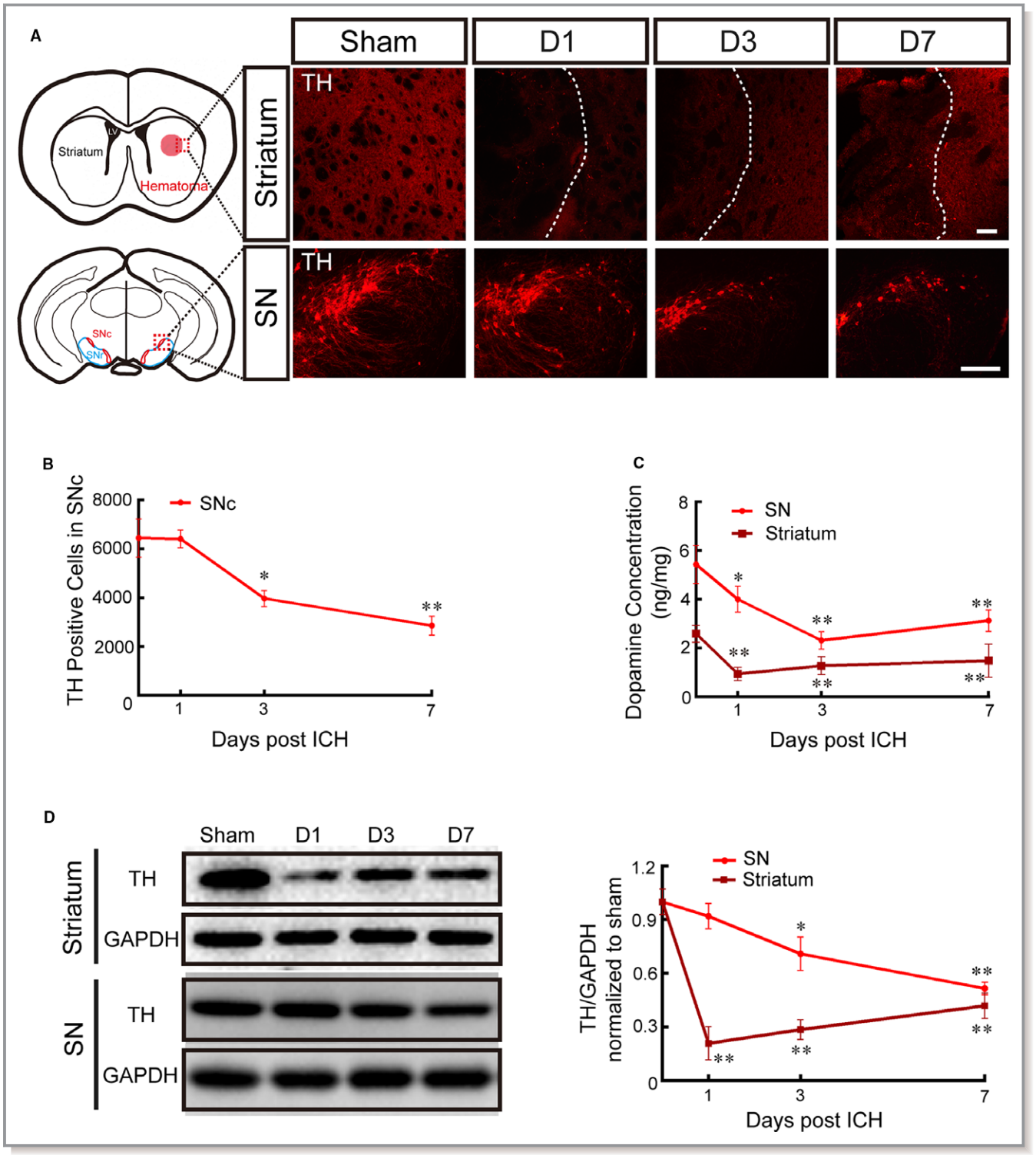

Figure 1. Striatal hemorrhage caused severe damage to dopamine neurons and fibers. A, Representative pictures of TH-labeled dopamine fibers and neurons in the striatum and the SN in the sham group and at 1, 3, and 7 days after ICH (scale bar=100 μm; red dotted grid indicates the observation area, and white dotted lines distinguish the hematoma area and the surrounding unaffected tissues). B, The number of TH-positive cells in the SNc was evaluated by stereology analysis at 1, 3, and 7 days after ICH and in the sham group (replaced by 0 days). C, The dopamine concentration in the striatum and the SN was measured using high-performance liquid chromatography–electrochemical detection at 1, 3, and 7 days after ICH and in the sham group (replaced by 0 day). D, Representative Western blot images and quantitative data of TH expression in the striatum and the SN at 1, 3, and 7 days after ICH and in the sham group (replaced by 0 days). Data are shown as mean±SEM (at least n=6 for each group; **P*<0.05 and ***P*<0.01 vs sham group). D indicates day; ICH, intracerebral hemorrhage; LV, lateral ventricle; SN, substantia nigra; SNc, substantia nigra pars compacta; TH, tyrosine hydroxylase.

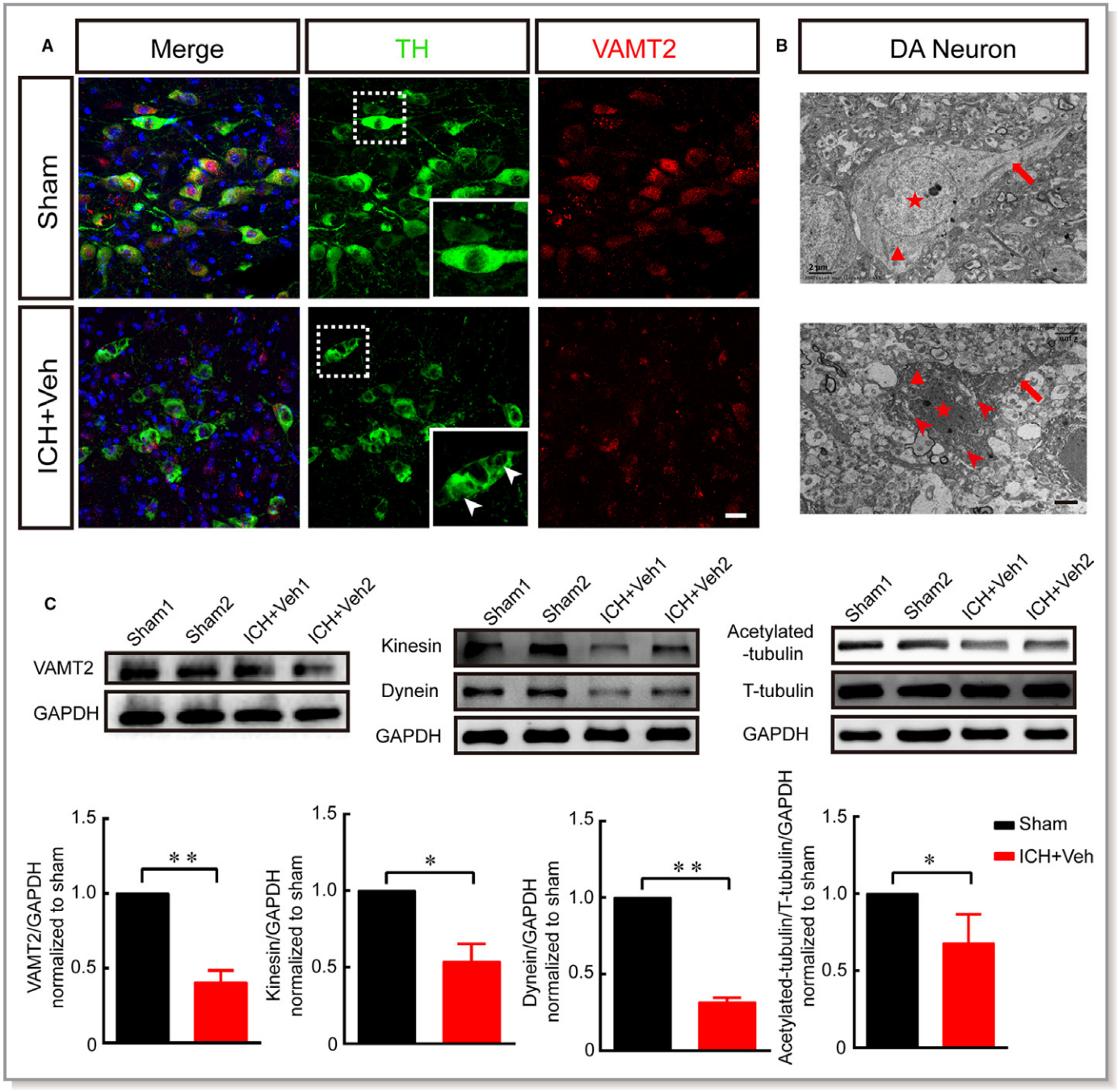

Figure 2. Microtubule depolymerization contributed to DA neuron impairment after ICH. A, Representative double immunofluorescence staining for TH and VMAT2 at 7 days after ICH (white arrowheads indicate vacuolated pathological changes; scale bar=20 μm); VMAT2 indicated the existence of vesicles capable of transporting monoamine neurotransmitters. B, Transmission electron micrographs showing the ultrastructure of DA neurons in the substantia nigra pars compacta 7 days after striatum hemorrhage (red asterisks indicate the DA neuron nucleus; red triangles indicate the cytoplasm; red arrowheads indicate vacuolated pathological changes; red arrows indicate the axon; scale bar=2 μm). C, Representative Western blot images and quantitative data of VMAT2, kinesin, dynein, and acetylated-tubulin protein expression in the substantia nigra of the sham and ICH+Veh groups at 7 days after ICH. Data are shown as mean±SEM (at least n=6 for each group; **P*<0.05 and ***P*<0.01 vs sham group). DA indicates dopamine; ICH, intracerebral hemorrhage; TH, tyrosine hydroxylase; Veh, vehicle; VMAT2, vesicular monoamine transporter 2.

ipsilateral SNc (≈ −2.92 to −3.64 from the bregma; 24 total sections available). The sum of the TH-positive cells was calculated by adding the TH-positive cells in each selected section.

TH-positive fibers in the basal ganglia surrounding the lesion and the ipsilateral SN pars reticulata as well as BDA-positive fibers in the striatum were quantitated according to optical density with KS300 software (AxioVision), as

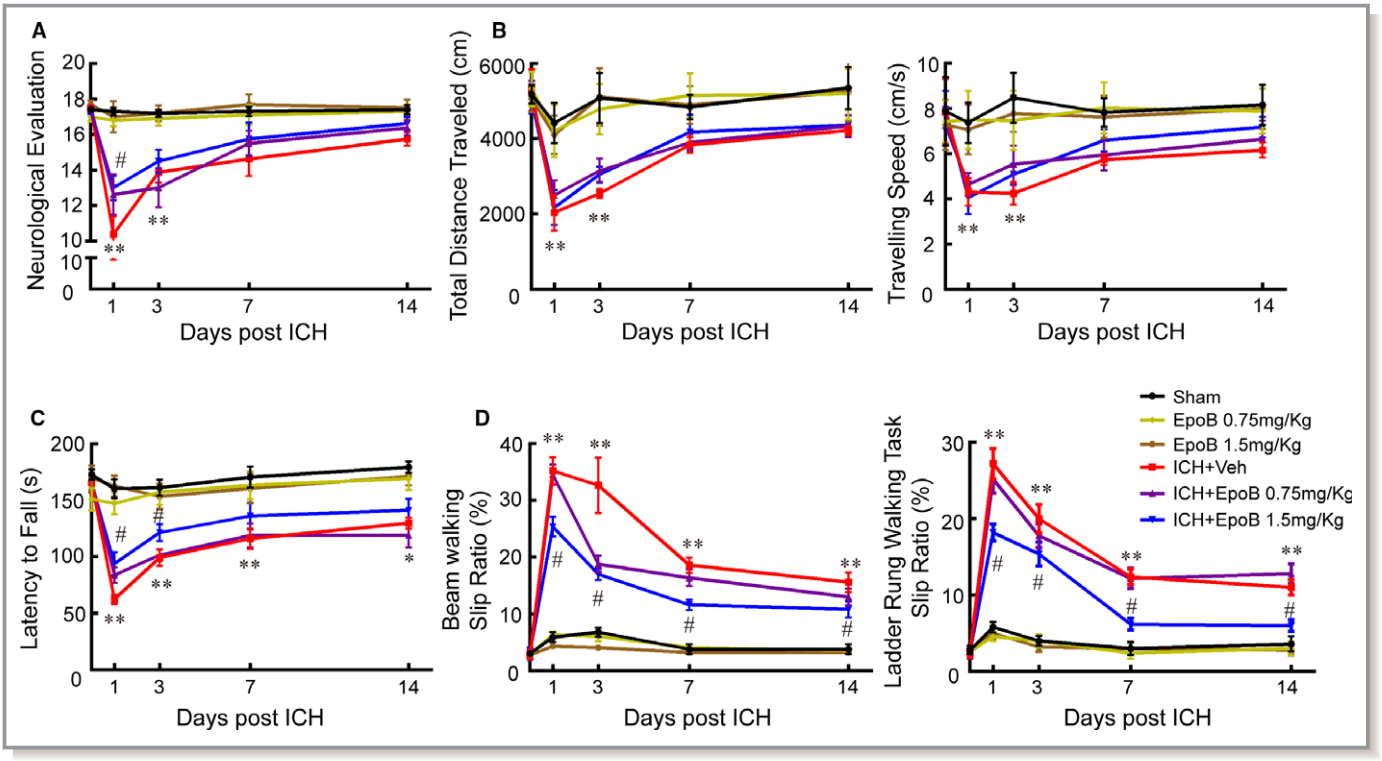

Figure 3. Systemic administration of epoB improved motor function after ICH. A, Somatosensory movement function was analyzed by neurological evaluation (18-point scale assessing the severity of impairment). B, General motor function was measured using the open-field test, and total distance traveled and traveling speed were recorded over a period of 10 minutes. C, Gross motor deficits were measured using the rotarod test, and the latency to fall was calculated for analysis. D, Fine motor function was tested using the beam-walking test and the ladder-rung walking task; the slip ratio of the contralateral limbs was counted within 50 steps (*P<0.05 and **P<0.01 of sham vs ICH+Veh group, $^{\#}P$<0.05 of ICH+Veh group vs ICH+epoB 1.5 mg/kg group). Data are shown as mean±SEM, at least n=10 for the behavior tests in each group. EpoB indicates epothilone B; ICH, intracerebral hemorrhage; Veh, vehicle.

described by Bao et al.[27] The relative optical density was obtained by subtracting the background optical density from the measured optical density. Then, the relative optical density of each group was normalized to that of the sham group and statistically analyzed using SPSS software (IBM Corp). The neurite length of the dopamine neurons on the coverslips were photographed and measured using ImageJ software, and at least 100 cells per mouse were measured.

Each experimental group included 5 mice, and at least 4 frozen sections were analyzed for each mouse, all of which were assessed in a double-blind manner.

Statistical Analyses

Statistical analysis was performed using SPSS 18.0 software. Data were expressed as the mean±SEM. Comparisons between 2 groups were analyzed using 2-tailed Student t tests. Number of dopamine neurons, dopamine concentration, Western blot, and behavioral data collected at repeating time points were analyzed using 2-way repeated-measures ANOVA, followed by the Bonferroni post hoc test. Other data for Western blot, optical density, and cell proportion were analyzed using 1-way ANOVA (1 factor) followed by the Scheffe post hoc test. P<0.05 was considered statistically significant.

Results

Intrastriatal Hemorrhage Resulted in Severe Damage to the Nigrostriatal Pathway

The pathological lesions in the nigrostriatal pathway in the striatum and SN were analyzed during the acute stage after ICH. Impaired TH-positive dopamine fibers and neurons in the striatum and SN were detected from 1 to 7 days after ICH (Figure 1A). In addition, these morphological results were supported by the levels of TH protein expression detected using Western blotting (Figure 1D). Furthermore, the dopamine concentration also significantly decreased in the striatum and SN areas following ICH (sham group, 1, 3, and 7 days, SN area: 5.43±0.78, 4.01±0.53, 2.31±0.36, and 3.13±0.44 ng/mg, respectively; striatum: 2.6±0.35, 0.94±0.27, 1.28±0.37, and 1.48±0.68 ng/mg, respectively;

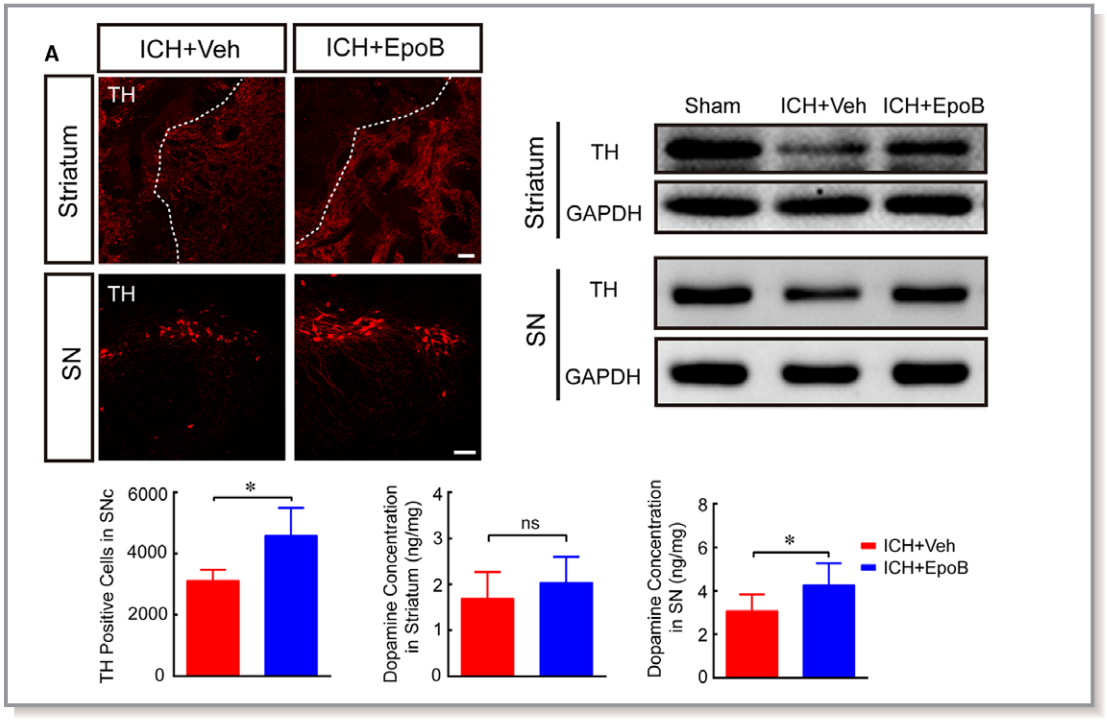

Figure 4. Systemic administration of epoB rescues DA neuron and fiber impairment by promoting microtubule stabilization. A, Representative immunofluorescence staining of TH in the striatum and the SN of the ICH+Veh and ICH+epoB groups 7 days after ICH (scale bar=100 μm); TH protein expression was also verified using Western blotting. Quantitative data (below) of the TH-positive cell number in the SNc and DA concentration in the SN and the striatum for the ICH+Veh and ICH+epoB groups. B, Representative double immunofluorescence staining of TH and VMAT2 in the SN of the ICH+Veh and ICH+epoB groups 7 days after ICH (white arrowheads indicate vacuolated pathological changes; scale bar=20 μm). C, Transmission electron micrographs showing the morphology of DA neurons in the SNc 7 days after ICH (red asterisks indicate the DA neuron nucleus; red triangles indicate the cytoplasm; red arrowheads indicate vacuolated pathological changes; red arrows indicate the axon; scale bar=2 μm). D, Representative Western blot images and quantitative data of VMAT2, kinesin, dynein, and acetylated-tubulin protein expression in the SN of the sham, ICH+Veh and ICH+epoB groups at 7 days after ICH. Data are shown as mean±SEM (at least n=6 for each group; *P<0.05). DA, dopamine; epoB indicates epothilone B; ICH, intracerebral hemorrhage; ns, not significant; SN indicates substantia nigra; SNc, substantia nigra pars compacta; TH, tyrosine hydroxylase; Veh, vehicle; VMAT2, vesicular monoamine transporter 2.

Figure 1C). Numbers of TH-positive cells in the SNc were counted using a stereological method, and significant damage was apparent at 3 and 7 days during the acute stage after ICH (sham group, 6449±788; 1 day, 6407±367; 3 days, 3975±324; 7 days, 2864±387; Figure 1B).

Microtubule Depolymerization Contributed to Dopamine Neuron Impairment After ICH

To investigate the pathomorphological changes of dopamine neurons after striatal hemorrhage, high-resolution immunofluorescence and electron microscopy were used. Interestingly, the soma of dopamine neurons presented vacuolated pathological changes 7 days after ICH (Figure 2A and 2B). In addition, VMAT2 expression (40.51±8.12% of sham group; P=0.002) was significantly decreased in dopamine neurons 7 days after ICH, as detected by immunofluorescence and Western blotting (Figure 2A and 2C), indicating the existence of an axonal transport barrier and low dopamine concentrations in dopamine neurons. Similarly, the expression of kinesin (53.64±11.63% of sham group; P=0.026), dynein (31.62±3.25% of sham group; P=0.001), and acetylated α-tubulin (67.86±18.97% of sham group; P=0.038; Figure 2C) also significantly decreased after ICH (Figure 2C), indicating depolymerized and unstable microtubules and axonal transport barriers.

Systemic Administration of EpoB Improved Behavioral Performance After ICH and Exerted No Side Effects in Mice

Different concentrations were used to examine the effectiveness and safety of systemic epoB administration. EpoB injection at concentrations of 0.75 and 1.5 mg/kg had no

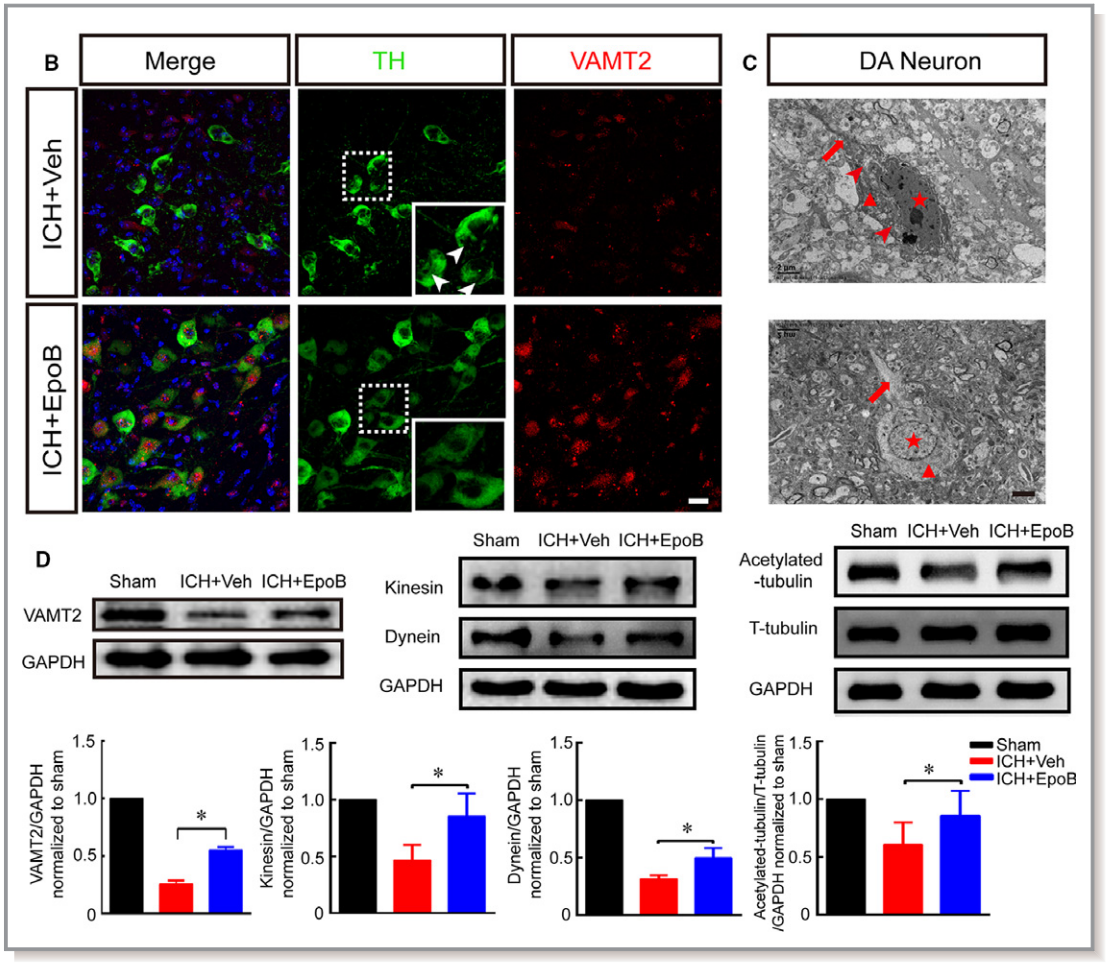

Figure 4. Continued

apparent influence on the number of white blood cells (Figure S1) or motor function (Figure 3A through 3D) at 1, 3, 7, and 14 days compared with the control group. However, a high concentration of 3.0 mg/kg induced a remarkable decrease in the number of white blood cells at 1, 3, and 7 days after injection (Figure S1). The ICH group exhibited significant decreases in body weight and survival rate compared with the sham group, but eopB treatment did not alleviate the body weight and survival rate compared with ICH+Veh group (Figure S1). Compared with the sham group, the ICH+Veh group showed significantly impaired neurological function and open-field performance (total distance traveled and traveling speed) at 1 and 3 days after ICH, and 1.5 mg/kg epoB apparently improved the neurological evaluation at only 1 day after ICH (Figure 3A and 3B). Regarding gross motor function, ICH led to shorter fall latency in the rotarod test compared with the sham group from 1 to 14 days after ICH, and 1.5 mg/kg epoB alleviated the decreased fall latency at only 1 and 3 days after ICH (Figure 3C). Regarding fine motor function, the slip ratios of the beam and ladder-rung walking tasks were significantly increased in the ICH+Veh group from 1 to 14 days after ICH. Surprisingly, 1.5 mg/kg epoB rescued the slip ratios during the acute and chronic stages (Figure 3D).

Systemic Administration of EpoB Ameliorated Nigrostriatal Pathway Impairment by Promoting Microtubule Stabilization

After examining the protective effects of epoB in motor function, we detected the effects of 1.5 mg/kg epoB on dopamine neuron and fiber morphology. EpoB treatment significantly increased TH-positive dopamine neurons (4599±896 versus 3125±356; P=0.034) in SN and TH-positive fibers in the striatum compared with the ICH+Veh group. Those morphological results were also supported by TH protein expression levels detected using Western blotting. EpoB treatment significantly increased the dopamine concentration in SN areas (4.28±0.99 versus 3.08±0.75 ng/mg; P=0.041) compared with the dopamine concentration in SN areas of the ICH+Veh group (Figure 4A). Furthermore, epoB treatment also alleviated the vacuolated pathological changes

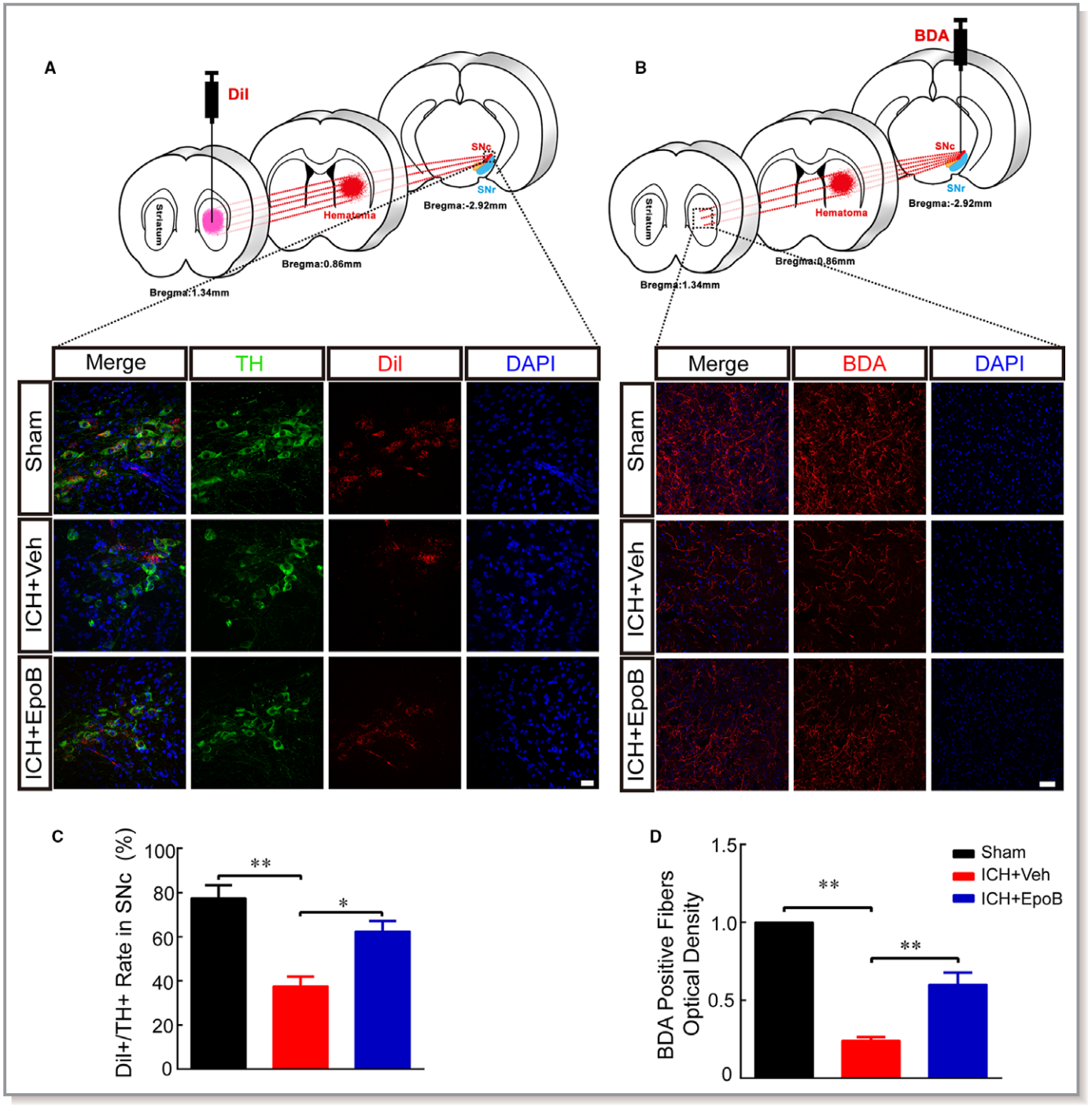

Figure 5. EpoB treatment alleviates nigrostriatal neural circuit impairment after ICH. A, Schematic diagram illustrating the experimental procedures of participating retrograde neural circuit tracking using DiI and representative double immunofluorescence staining of TH and DiI at the SNc (scale bar=20 μm) 7 days after ICH. B, Schematic diagram illustrating the experimental procedures of participating anterograde neural circuit tracking using BDA and representative immunofluorescence staining of BDA-positive fibers in the striatum (scale bar=50 μm) 14 days after ICH. C, Proportion of DiI-labeled neurons among TH-positive neurons for the 3 groups. D, Quantification of the optical density of the BDA-positive fibers. Data are shown as mean±SEM (at least n=6 for each group; *P<0.05 and **P<0.01). BDA indicates biotin dextran amine; DAPI, 4′,6-diamidino-2-phenylindole; epoB indicates epothilone B; ICH, intracerebral hemorrhage; SNc, substantia nigra pars compacta; TH, tyrosine hydroxylase; Veh, vehicle.

in dopamine neurons caused by ICH as assessed using high-resolution immunofluorescence and electron microscopy (Figure 4B and 4C). The levels of acetylated α-tubulin were apparently increased in the ICH + epoB group compared with the ICH+Veh group, indicating that the epoB treatment group had more stable microtubules (Figure 4D). Furthermore,

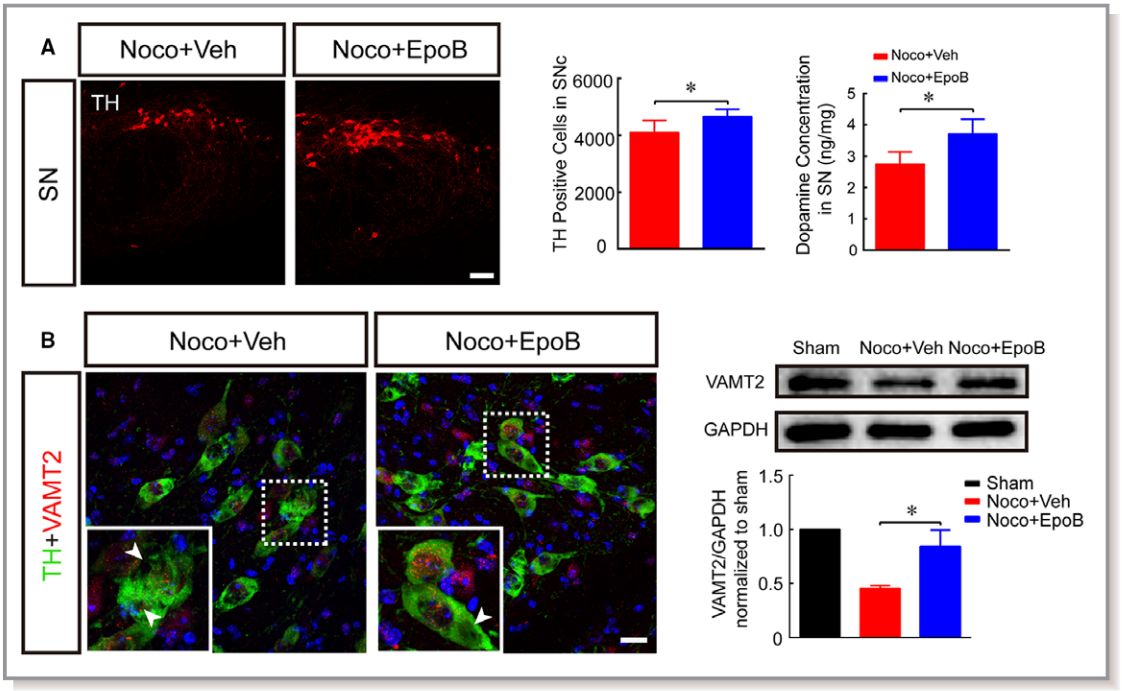

Figure 6. Intrastriatal injection of Noco partly simulated the pathological characteristics of ICH. A, Representative immunofluorescence staining of TH in SN 7 days after Noco injection (scale bar=100 μm). The number of TH-positive cells in the SNc and dopamine concentration were measured in the SN 7 days after Noco injection. B, Representative double immunofluorescence staining for TH and VMAT2 7 days after Noco injection (white arrowheads indicate vacuolated pathological changes; scale bar=20 μm), representative Western blot images and quantitative data of VMAT2 for SN tissues from the Noco+Veh and Noco+epoB groups. C, Representative double immunofluorescence staining (left) and quantitative data (right) of TH and DiI at the SNc (scale bar=20 μm) 7 days after Noco injection. D, Immunofluorescence staining of BDA-positive fibers (left) and optical density quantitative data (right) at the striatum (scale bar=50 μm) 14 days after Noco injection. E, Quantitative study of the open-field, rotarod, and beam-walking tests in mice of the Noco+Veh and Noco+epoB groups. Data are shown as mean±SEM (at least n=6 for each group; **P*<0.05 and ***P*<0.01). BDA indicates biotin dextran amine; epoB, epothilone B; ICH, intracerebral hemorrhage; Noco, nocodazole; SN, substantia nigra; SNc, substantia nigra pars compacta; TH, tyrosine hydroxylase; Veh, vehicle; VMAT2, vesicular monoamine transporter 2.

intracellular axonal transport function was apparently improved in the ICH + epoB group, as indicated by the increased expression of kinesin, dynein, and VMAT2 (Figure 4B and 4D).

To detect the structural and functional integrity of the nigrostriatal pathway, anterograde and retrograde neural circuit tracking methods were used (schematic diagrams illustrating the experimental procedures are shown in Figure 5A and 5B). We found that ICH caused a significant decrease in the number of DiI-labeled TH-positive dopamine neurons; however, epoB treatment remarkably increased the ratio of DiI-labeled TH-positive dopamine neurons (62.48±4.65% versus 37.6±4.37%; *P*=0.046) in the SNc (Figure 5A and 5C). Furthermore, the optical density of BDA-positive fibers in the striatum was significantly lower in the ICH+Veh group than in the sham group, whereas epoB administration apparently increased the optical density (0.6±0.07 versus 0.24±0.02; *P*=0.003) of the dopamine fibers (Figure 5B and 5D).

Intrastriatal Injection of Nocodazole Partially Simulated the Pathological Characteristics of ICH

We established a model of intrastriatal injection of nocodazole to ensure that microtubule depolymerization was a pivotal process in nigrostriatal pathway impairment after ICH. Nocodazole injection led to severe motor dysfunction in the open-field, rotarod, and beam-walking tests at 7 days after injection, but epoB treatment remarkably improved motor ability compared with that of the nocodazole + vehicle group (Figure 6E). Similarly, epoB treatment significantly increased the number of dopamine neurons (4672±252 versus 4116±416; *P*=0.048) and the dopamine concentration (3.71±0.47 versus 2.75±0.29 ng/mg; *P*=0.02) in the SN at 7 days after injection compared with the levels of the nocodazole + vehicle group (Figure 6A). Regarding the microstructure, nocodazole induced vacuolated pathological changes in the dopamine neurons, but more complete dopamine neuronal structures were found in the epoB

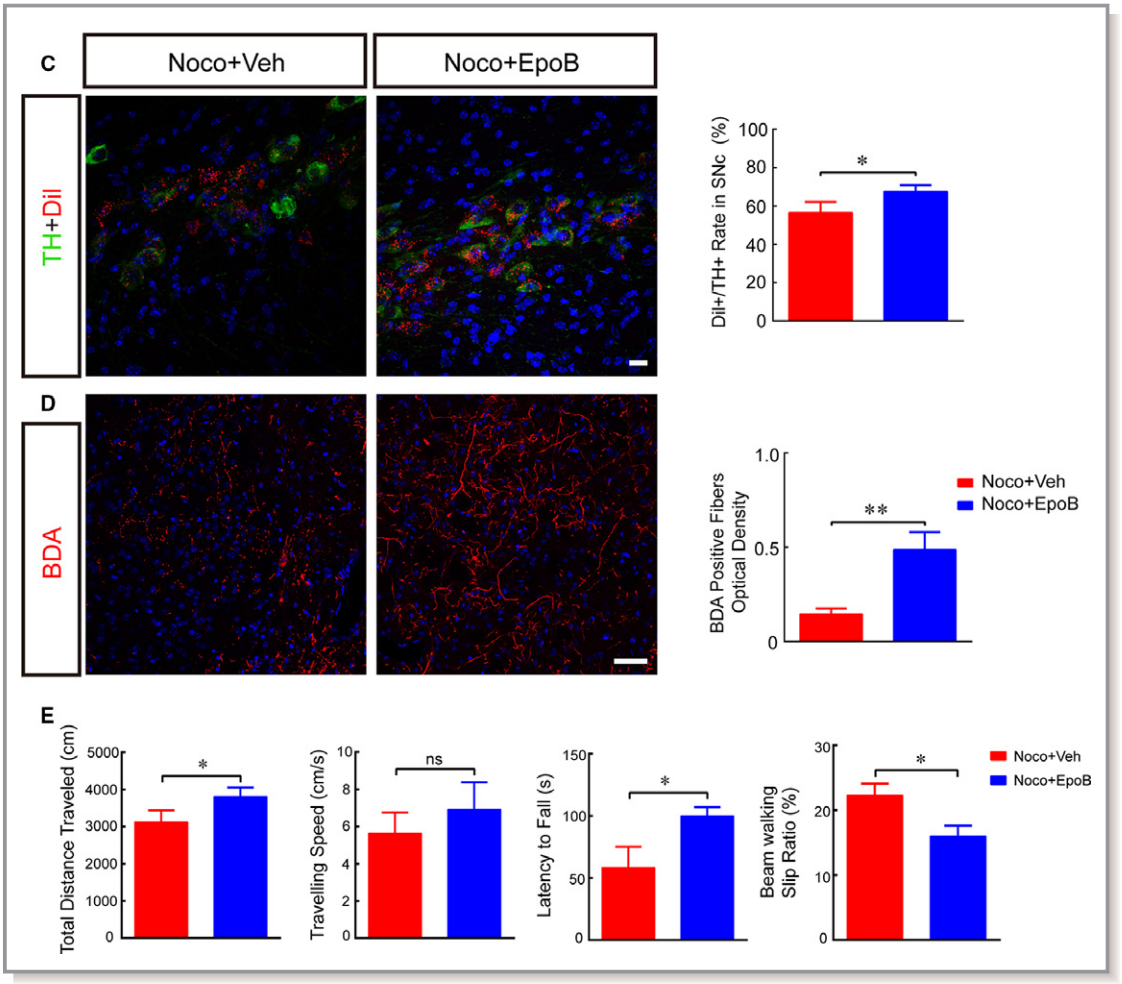

Figure 6. Continued

treatment group (Figure 6B). Moreover, fewer VMAT2-positive vesicles were detected in the nocodazole + vehicle group compared with the nocodazole + epoB group (Figure 6B). The Dil^+/TH^+ dopamine neuron ratio in the SNc and the optical density of the BDA-positive fibers in the striatum were significantly decreased in the nocodazole + vehicle group, but epoB treatment improved the structural and functional integrity of nigrostriatal projections by increasing the Dil^+/TH^+ dopamine neuron ratio (67.5±3.37% versus 56.4±5.58%; P=0.035) and the optical density of BDA-positive fibers (0.49±0.09 versus 0.15±0.03; P=0.001; Figure 6C and 6D).

EpoB Maintained Microtubule Stability by Increasing the Expression of Acetylated α-Tubulin In Vivo and In Vitro

Previous studies have demonstrated that αTAT1 is a specific acyltransferase that promotes α-tubulin acetylation on lysine 40 (K40); thus, we designed 3 shRNA constructs to interfere with the expression of αTAT1. After testing the interference efficiency of the shRNAs (Figure S2A and S2B), the scrambled shRNA and shRNA2 (interference efficiency 90.8%) were used in the subsequent experiments. Acetylated α-tubulin expression and the number of dopamine neurons were significantly decreased after injection of human B lymphotropic virus–αTAT1 shRNA (Figure 7A through 7C), and local injection of epoB also increased the expression of acetylated α-tubulin and rescued dopamine neurons that were lose after ICH (Figure 7B and 7C). However, epoB had no function beneficial to acetylated α-tubulin and dopamine neurons after injection of human B lymphotropic virus–αTAT1 shRNA (Figure 7B and 7C). Furthermore, acetylated α-tubulin expression of neurons from SN was apparently decreased in the group treated with oxyhemoglobin, a decomposition product of autologous blood, but this impairment could be alleviated by epoB treatment (Figure 7D and 7E). In cells administered αTAT1 shRNA, epoB treatment exerted no protective effects against reduced acetylated α-tubulin expression due to oxyhemoglobin treatment (Figure 7D and 7E). We demonstrated that epoB maintained microtubule stability associated with increased expression of acetylated α-tubulin.

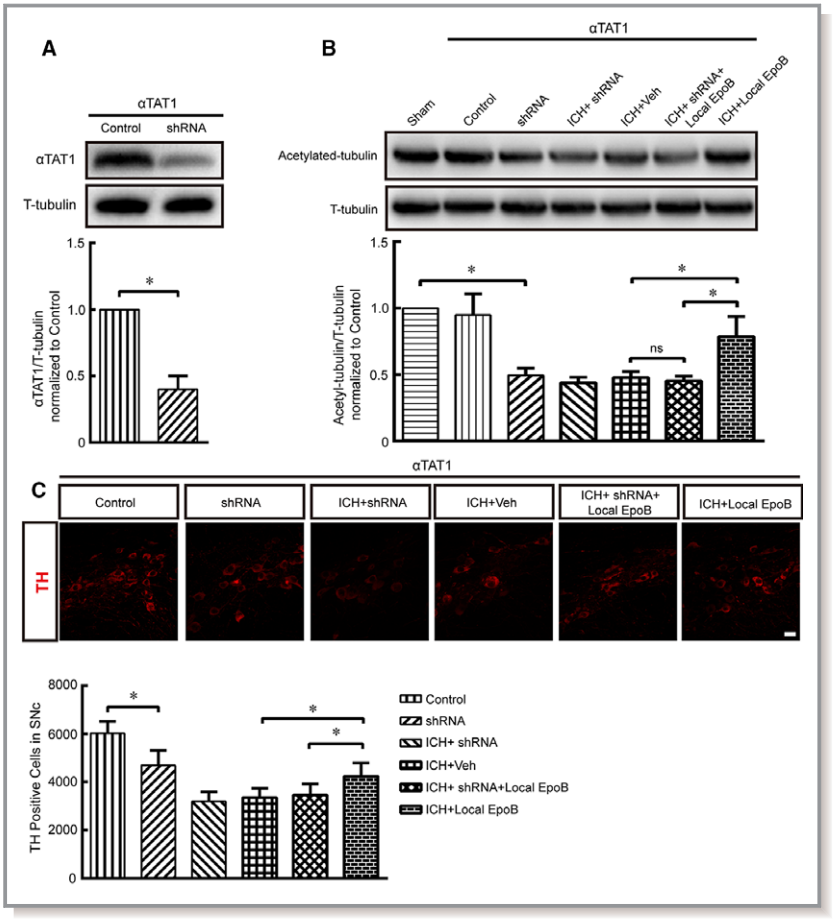

Figure 7. EpoB maintained microtubule stability by increasing the expression of acetylated α-tubulin in vivo and in vitro. A, Representative Western blot images and quantitative data of αTAT1 expression after shRNA interference. B, Representative Western blot images and quantitative data of acetylated α-tubulin expression of the sham, control shRNA, shRNA, ICH+shRNA, ICH+Veh, ICH+shRNA+local epoB and ICH+local epoB groups in vivo. C, Representative immunofluorescence staining and quantitative data of TH-positive dopamine neurons in the SN 7 days after shRNA interference and epoB treatment (scale bar=20 μm). D and E, Representative immunofluorescence images (D, scale bar=20 μm), Western blot images, and quantitative data (E) of acetylated α-tubulin and total α-tubulin expression of control, epoB, OH, and OH+epoB groups under different shRNA conditions in SN neurons. Data are shown as mean±SEM (at least n=6 for each group; **P*<0.05 and ***P*<0.01). DAPI indicates 4′,6-diamidino-2-phenylindole; epoB, epothilone B; ICH, intracerebral hemorrhage; ns, not significant; OH indicates oxyhemoglobin; shRNA, short hairpin RNA; SN, substantia nigra; Veh, vehicle.

Discussion

In this study, we found that intrastriatal hemorrhage significantly impaired the nigrostriatal pathway (including dopamine neurons and nigrostriatal projection fibers) and deteriorated motor function and axoplasmic transport after ICH by promoting microtubule depolymerization. In addition, epoB alleviated nigrostriatal pathway injury and improved motor function associated with microtubule stabilization by increasing the expression of acetylated α-tubulin (Figure 8, schematic diagram).

Motor dysfunction resulting from ICH is a devastating outcome that severely disrupts patients' quality of life, and no effective therapies are available. Our previous study demonstrated that targeted protection of white matter fibers in the pyramidal system against injury could only partially alleviate motor deficiency after ICH; this indicated that integrated motor circuit protection is also involved. The motor circuit includes the pyramidal and extrapyramidal systems, both of which elaborately and cooperatively produce accurate motor function.[4] The nigrostriatal pathway, which is part of the extrapyramidal system, plays an important role in controlling

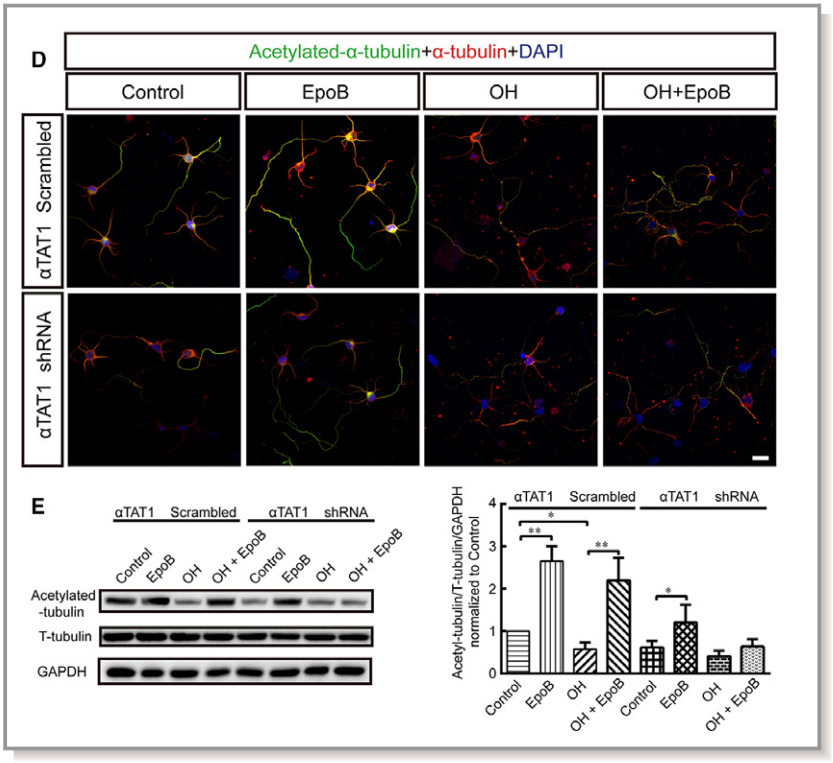

Figure 7. Continued

movement. Clinical and animal studies found that nigrostriatal dopamine neurons and fibers were vulnerable to microtubule disruption, ischemic stroke, and traumatic brain injury, and parkinsonism locomotor dysfunction was a late-onset symptom associated with these injuries,[10,28–30] indicating that microtubules in dopamine neurons may be a target of nigrostriatal vulnerability. Our findings confirmed and substantially expanded the results of these previous studies by demonstrating that ICH could lead to nigrostriatal pathway damage and motor dysfunction, and dopamine neurons in the SN presented vacuolated pathological changes. These pathological lesions could also be induced by intrastriatal injection of nocodazole. Our results revealed that the nigrostriatal pathway undergoes severe impairment after ICH via microtubule depolymerization. This is a significant discovery that extends our limited knowledge to better reflect the pathological changes of the nigrostriatal pathway after ICH. Interestingly, systemic administration of the microtubule stabilizer epoB promoted microtubule stabilization, significantly alleviated nigrostriatal pathological injury, and improved coordination ability (as assessed using the rotarod, beam, and ladder-rung walking tasks), which is consistent with investigations that showed epoB treatment of Alzheimer disease and spinal cord injury promoted microtubule stabilization and axonal regeneration.[11–13] In addition, there were no apparent side effects of epoB systemic administration, making epoB a promising candidate for clinical testing. These results suggested that microtubule-targeted treatment can protect against pathological changes in dopamine neurons induced by ICH and that additional research on motor recovery after ICH requires more focus not only in the pyramidal system but also in the extrapyramidal system.

In addition to their important role in providing structural support, healthy microtubules also serve as a scaffold for axonal transport, which is vital for neuronal physiological function. Moreover, kinesin and dynein are the main motor proteins that traffic intracellular cargo along microtubules, including vesicles, organelles, protein complexes, and mRNA.[31] Previous studies revealed that disassembling microtubules leads to dysfunction in kinesin- and dynein-driven axonal transport with central nervous system injury or neurodegenerative diseases, and this compromised axonal transport is closely associated with early neurological dysfunction in ICH.[32] Similarly, we found that expression of kinesin and dynein was significantly decreased following disruption of microtubules in damaged dopamine neurons; this indicates that axonal transport in the nigrostriatal pathway was damaged. VMAT2 is a transmembrane transporter protein that packages monoamine neurotransmitters, including dopamine, serotonin, and norepinephrine, into vesicles. Decreased expression of VMAT2 has been proven in psychiatric disorders, Parkinson disease, and other neurological disorders.[33] Surprisingly, immunostaining and immunoblotting results simultaneously verified that VMAT2 expression also decreased in dopamine neurons after

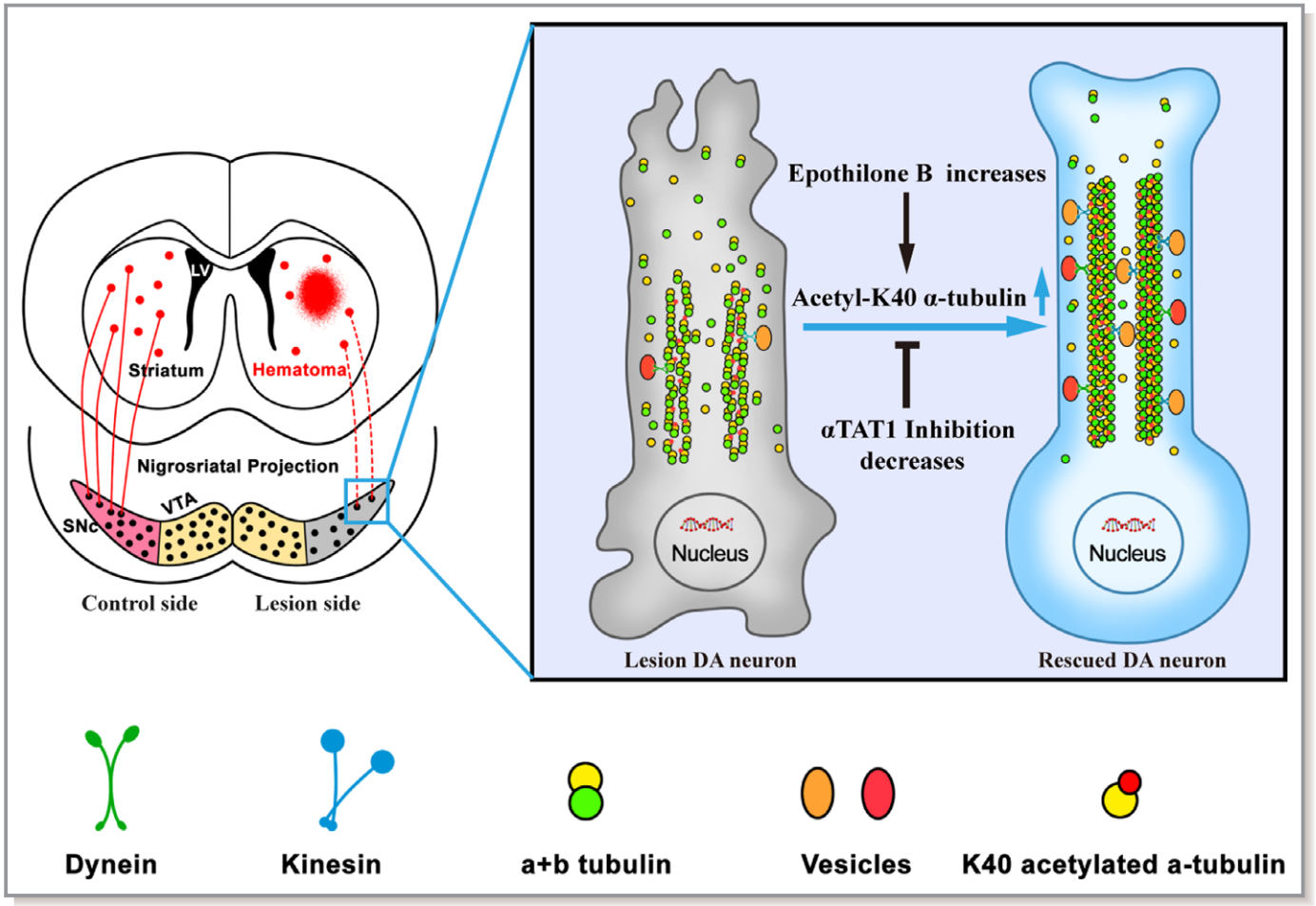

Figure 8. Schematic summary. Striatal hemorrhage–induced impairment of the nigrostriatal pathway, including DA neurons and projection fibers from the SN to striatum. Microtubule depolymerization was an important pathological factor in nigrostriatal pathway damage, which contributes to motor function deficits and blocked axoplasmic transport. The microtubule stabilizing agent epoB can alleviate pathological lesions in the nigrostriatal pathway and improve motor function by maintaining microtubule stability via increased expression of acetylated α-tubulin. DA indicates dopamine; epoB, epothilone B; LV, lateral ventricle; SN, substantia nigra; VTA, ventral tegmental area.

ICH and intrastriatal injection of nocodazole. However, treatment with the microtubule stabilizer epoB can alleviate axonal transport damage in nigrostriatal projections by increasing the expression levels of VMAT2. Moreover, anterograde and retrograde neural circuit tracking using DiI and BDA also demonstrated that the structural and functional integrity of the nigrostriatal pathway was apparently impaired by ICH and intrastriatal injection of nocodazole. However, epoB treatment stabilized the structural and functional integrity of the nigrostriatal pathway. These pathological changes and immunostaining results revealed that ICH could impair microtubule- and membrane-dependent axonal transport of nigrostriatal fiber projections in the striatum and SN, whereas epoB-induced microtubule stability can alleviate these deficits.

Acetylation is a reversible posttranslational modification that plays a fundamental role in the epigenetic regulation of gene expression.[34] Interestingly, αTAT1 (also known as MEC-17) is a specific acyltransferase that promotes α-tubulin acetylation on lysine 40 (K40), and many studies have verified that elevated levels of acetylated α-tubulin are a marker of stable microtubules.[35,36] Furthermore, this study also revealed that the loss of MEC-17 (αTAT1) expression leads to microtubule instability, axonal degeneration, and disrupted axonal transport in *Caenorhabditis elegans*.[37] In addition, MEC-17 (αTAT1) deficiency leads to reduced α-tubulin acetylation and impaired migration of cortical neurons in mice.[38] We found that αTAT1 knockdown by shRNA decreased the expression of acetylated α-tubulin in vivo and in vitro, which is consistent with the findings observed in *C. elegans*.[37] Furthermore, oxyhemoglobin treatment also decreased the acetylated α-tubulin expression of SN neurons (there were only 4.6% TH-positive dopamine cells in the primary SN culture system [Figure S3]), but epoB ameliorates oxyhemoglobin-induced impairments by increasing the expression of acetylated α-tubulin to maintain microtubule stability. However, when we knocked down acyltransferase

αTAT1 using shRNA, systematic and local injection of epoB had no protective effects for the neurons after ICH in vivo and oxyhemoglobin treatment in vitro. This evidence suggests that epoB authentically maintained microtubule stability by increasing acetylated α-tubulin expression.

Much work remains to be done in future studies. First, in this study, we explored only the protective effect of epoB in nigrostriatal pathway injury after ICH; however, epoB may also alleviate motor dysfunction by benefiting the recovery of other neural pathways after ICH. Consequently, the pathological changes of other neural pathways after ICH still need investigation. Second, the mechanism of the epoB protective effect revealed in the study was not clear. Genetically engineered mice are needed in future work to clarify the dominant mechanism by which epoB alleviates microtubule injury and motor dysfunction after ICH.

In summary, microtubule depolymerization contributed to impairment of dopamine neurons and nigrostriatal projection fibers after striatal hemorrhage. Treatment with epoB can alleviate pathological lesions in the nigrostriatal pathway and improve motor function, which was associated with microtubule stability via increasing expression of acetylated α-tubulin. This microtubule-targeted therapeutic strategy has translational promise for treating functional recovery after ICH, from bench to bedside.

Acknowledgments

We are grateful to Doctor Pengfei Wu from the Department of Neurosurgery, Daping Hospital, Third Military Medical University, Chongqing, China, for the generous academic advice related to this work.

Sources of Funding

This study was supported by the National Basic Research Program of China (973 Program, No. 2014CB541600) and the Basic Science and Advanced Technology Research Project of Chongqing (Grant No. cstc2016jcyjA1730).

Disclosures

None.

References

1. Xi G, Strahle J, Hua Y, Keep RF. Progress in translational research on intracerebral hemorrhage: is there an end in sight? *Prog Neurobiol*. 2014;115:45–63.
2. Hankey GJ. Stroke. *Lancet*. 2017;389:641–654.
3. Keep RF, Hua Y, Xi G. Intracerebral haemorrhage: mechanisms of injury and therapeutic targets. *Lancet Neurol*. 2012;11:720–731.
4. de Oliveira-Souza R. The human extrapyramidal system. *Med Hypotheses*. 2012;79:843–852.
5. Scheidtmann K, Fries W, Muller F, Koenig E. Effect of levodopa in combination with physiotherapy on functional motor recovery after stroke: a prospective, randomised, double-blind study. *Lancet*. 2001;358:787–790.
6. Rosser N, Heuschmann P, Wersching H, Breitenstein C, Knecht S, Floel A. Levodopa improves procedural motor learning in chronic stroke patients. *Arch Phys Med Rehabil*. 2008;89:1633–1641.
7. Ruscher K, Kuric E, Wieloch T. Levodopa treatment improves functional recovery after experimental stroke. *Stroke*. 2012;43:507–513.
8. Janke C, Kneussel M. Tubulin post-translational modifications: encoding functions on the neuronal microtubule cytoskeleton. *Trends Neurosci*. 2010;33:362–372.
9. Feng J. Microtubule: a common target for parkin and Parkinson's disease toxins. *Neuroscientist*. 2006;12:469–476.
10. Liang Y, Li S, Wen C, Zhang Y, Guo Q, Wang H, Su B. Intrastriatal injection of colchicine induces striatonigral degeneration in mice. *J Neurochem*. 2008;106:1815–1827.
11. Hellal F, Hurtado A, Ruschel J, Flynn KC, Laskowski CJ, Umlauf M, Kapitein LC, Strikis D, Lemmon V, Bixby J, Hoogenraad CC, Bradke F. Microtubule stabilization reduces scarring and causes axon regeneration after spinal cord injury. *Science*. 2011;331:928–931.
12. Sengottuvel V, Leibinger M, Pfreimer M, Andreadaki A, Fischer D. Taxol facilitates axon regeneration in the mature CNS. *J Neurosci*. 2011;31:2688–2699.
13. Ruschel J, Hellal F, Flynn KC, Dupraz S, Elliott DA, Tedeschi A, Bates M, Sliwinski C, Brook G, Dobrindt K, Peitz M, Brustle O, Norenberg MD, Blesch A, Weidner N, Bunge MB, Bixby JL, Bradke F. Axonal regeneration. Systemic administration of epothilone B promotes axon regeneration after spinal cord injury. *Science*. 2015;348:347–352.
14. Krafft PR, Rolland WB, Duris K, Lekic T, Campbell A, Tang J, Zhang JH. Modeling intracerebral hemorrhage in mice: injection of autologous blood or bacterial collagenase. *J Vis Exp*. 2012:e4289.
15. Rynkowski MA, Kim GH, Komotar RJ, Otten ML, Ducruet AF, Zacharia BE, Kellner CP, Hahn DK, Merkow MB, Garrett MC, Starke RM, Cho BM, Sosunov SA, Connolly ES. A mouse model of intracerebral hemorrhage using autologous blood infusion. *Nat Protoc*. 2008;3:122–128.
16. Erturk A, Hellal F, Enes J, Bradke F. Disorganized microtubules underlie the formation of retraction bulbs and the failure of axonal regeneration. *J Neurosci*. 2007;27:9169–9180.
17. Yang Y, Tang Y, Xing Y, Zhao M, Bao X, Sun D, Tang X, Wu Y, Xu H, Fan X. Activation of liver X receptor is protective against ethanol-induced developmental impairment of Bergmann glia and Purkinje neurons in the mouse cerebellum. *Mol Neurobiol*. 2014;49:176–186.
18. Xu P, Xu H, Tang X, Xu L, Wang Y, Guo L, Yang Z, Xing Y, Wu Y, Warner M, Gustafsson JA, Fan X. Liver X receptor beta is essential for the differentiation of radial glial cells to oligodendrocytes in the dorsal cortex. *Mol Psychiatry*. 2014;19:947–957.
19. Tan L, Ge H, Tang J, Fu C, Duanmu W, Chen Y, Hu R, Sui J, Liu X, Feng H. Amantadine preserves dopamine level and attenuates depression-like behavior induced by traumatic brain injury in rats. *Behav Brain Res*. 2015;279:274–282.
20. Seymour AB, Andrews EM, Tsai SY, Markus TM, Bollnow MR, Brenneman MM, O'Brien TE, Castro AJ, Schwab ME, Kartje GL. Delayed treatment with monoclonal antibody in-1 1 week after stroke results in recovery of function and corticorubral plasticity in adult rats. *J Cereb Blood Flow Metab*. 2005;25:1366–1375.
21. Curzon P, Zhang M, Radek RJ, Fox GB. Frontiers in neurosciencethe behavioral assessment of sensorimotor processes in the mouse: acoustic startle, sensory gating, locomotor activity, rotarod, and beam walking. In: Buccafusco JJ, ed. *Methods of Behavior Analysis in Neuroscience*. Boca Raton (FL): CRC Press/Taylor & Francis Taylor & Francis Group, LLC.; 2009:171–176.
22. Metz GA, Whishaw IQ. The ladder rung walking task: a scoring system and its practical application. *J Vis Exp*. 2009;28:e1204.
23. Fox GB, Fan L, Levasseur RA, Faden AI. Sustained sensory/motor and cognitive deficits with neuronal apoptosis following controlled cortical impact brain injury in the mouse. *J Neurotrauma*. 1998;15:599–614.
24. Fath T, Ke YD, Gunning P, Gotz J, Ittner LM. Primary support cultures of hippocampal and substantia nigra neurons. *Nat Protoc*. 2009;4:78–85.
25. Ge H, Yu A, Chen J, Yuan J, Yin Y, Duanmu W, Tan L, Yang Y, Lan C, Chen W, Feng H, Hu R. Poly-L-ornithine enhances migration of neural stem/progenitor cells via promoting alpha-Actinin 4 binding to actin filaments. *Sci Rep*. 2016;6:37681.
26. Masoud ST, Vecchio LM, Bergeron Y, Hossain MM, Nguyen LT, Bermejo MK, Kile B, Sotnikova TD, Siesser WB, Gainetdinov RR, Wightman RM, Caron MG, Richardson JR, Miller GW, Ramsey AJ, Cyr M, Salahpour A. Increased expression of the dopamine transporter leads to loss of dopamine neurons, oxidative stress and l-DOPA reversible motor deficits. *Neurobiol Dis*. 2015;74:66–75.

27. Bao X, Cai Y, Wang Y, Zhao J, He X, Yu D, Huang J, Jing S, Du Z, Yang T, Warner M, Gustafsson JA, Fan X. Liver X receptor beta is involved in formalin-induced spontaneous pain. *Mol Neurobiol*. 2017;54:1467–1481.
28. Borlongan CV, Cahill DW, Sanberg PR. Locomotor and passive avoidance deficits following occlusion of the middle cerebral artery. *Physiol Behav*. 1995;58:909–917.
29. Kizony R, Levin MF, Hughey L, Perez C, Fung J. Cognitive load and dual-task performance during locomotion poststroke: a feasibility study using a functional virtual environment. *Phys Ther*. 2010;90:252–260.
30. Lin PY, Chen JJ, Lin SI. The cortical control of cycling exercise in stroke patients: an fNIRS study. *Hum Brain Mapp*. 2013;34:2381–2390.
31. Lu W, Gelfand VI. Moonlighting motors: kinesin, dynein, and cell polarity. *Trends Cell Biol*. 2017;7:505–514.
32. Bradke F, Fawcett JW, Spira ME. Assembly of a new growth cone after axotomy: the precursor to axon regeneration. *Nat Rev Neurosci*. 2012;13:183–193.
33. Esteves AR, Cardoso SM. LRRK2 at the crossroad between autophagy and microtubule trafficking: insights into Parkinson's disease. *Neuroscientist*. 2016;23:16–26.
34. Song Y, Brady ST. Post-translational modifications of tubulin: pathways to functional diversity of microtubules. *Trends Cell Biol*. 2015;25:125–136.
35. Shida T, Cueva JG, Xu Z, Goodman MB, Nachury MV. The major alpha-tubulin K40 acetyltransferase alphaTAT1 promotes rapid ciliogenesis and efficient mechanosensation. *Proc Natl Acad Sci USA*. 2010;107:21517–21522.
36. Akella JS, Wloga D, Kim J, Starostina NG, Lyons-Abbott S, Morrissette NS, Dougan ST, Kipreos ET, Gaertig J. MEC-17 is an alpha-tubulin acetyltransferase. *Nature*. 2010;467:218–222.
37. Neumann B, Hilliard MA. Loss of MEC-17 leads to microtubule instability and axonal degeneration. *Cell Rep*. 2014;6:93–103.
38. Li L, Wei D, Wang Q, Pan J, Liu R, Zhang X, Bao L. MEC-17 deficiency leads to reduced alpha-tubulin acetylation and impaired migration of cortical neurons. *J Neurosci*. 2012;32:12673–12683.

SUPPLEMENTAL MATERIAL

Figure S1. The effect on white blood cell, body weight and percent survival of systemic administration of EpoB.

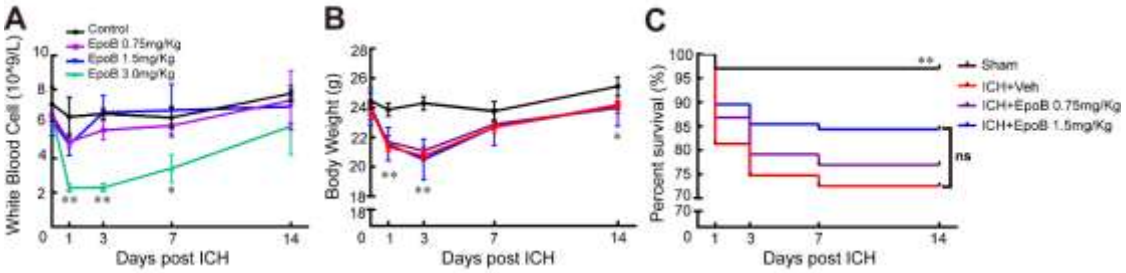

A, White blood cell counts at different EpoB concentrations (0, 0.75 mg/kg, 1.5 mg/kg and 3.0 mg/kg) and different times ($^{*}P<0.05$ and $^{**}P<0.01$ of 3.0 mg/kg versus the control group). **B,** Body weight changes measured at 0, 1, 3, 7, and 14 days post-ICH. **C,** Survival rate at 0, 1, 3, 7, and 14 days post-ICH. Data are shown as the means ± SEM (at least n=6 for each group; $^{*}P<0.05$ and $^{**}P<0.01$).

Figure S2. The interference efficiency of αTAT1 shRNAs tested by QPCR and western blotting.

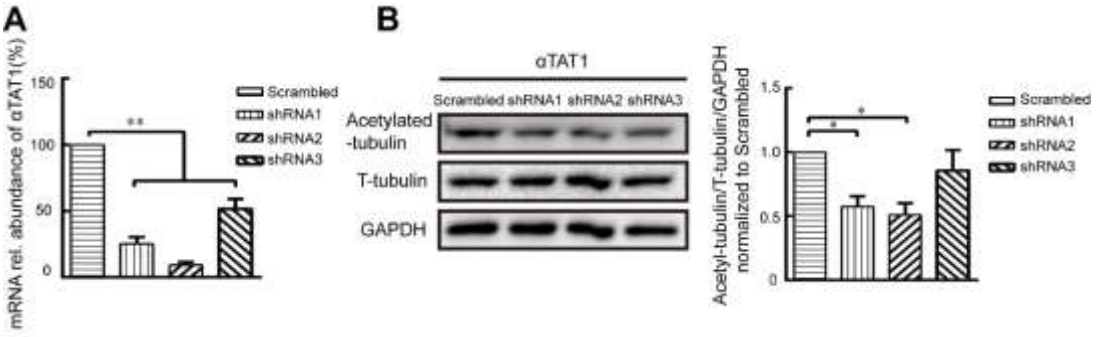

A, Relative mRNA abundance of αTAT1 after shRNA treatment. **B,** The protein expression levels of acetylated-α-tubulin after treatment with αTAT1 shRNAs.

Figure S3. Identification of DA neurons from primary SN neurons by TH staining.

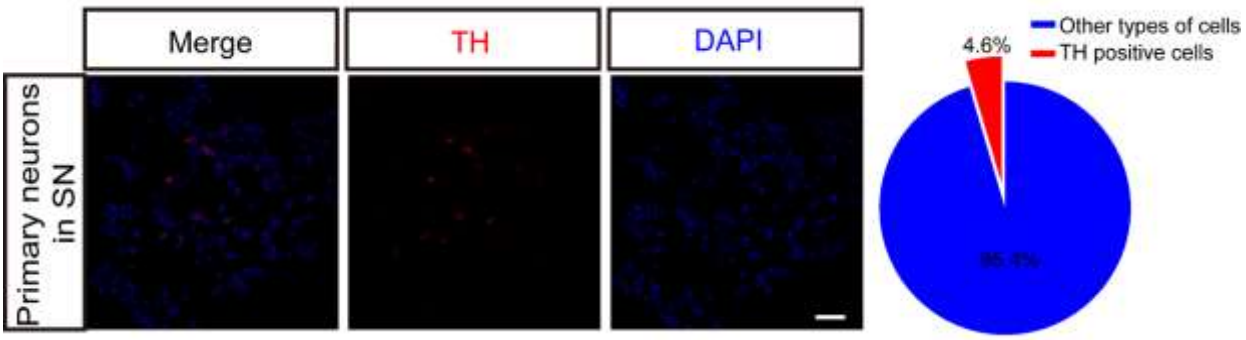

Representative fluorescent images (left) and quantitative date (right) for TH and DAPI staining. Scale bar, 50μm.